JOURNAL OF CATALYSIS 64, 18–28 (1980)

Solid Electrolyte Aided Study of the Ethylene Oxide Oxidation on Silver

MICHAEL STOUKIDES AND COSTAS G. VAYENAS

Massachusetts Institute of Technology, Cambridge, Massachusetts 02139

Received July 2, 1979; revised January 29, 1980

The oxidation of ethylene oxide on polycrystalline Ag films supported on stabilized zirconia was studied in a CSTR at atmospheric pressure and temperatures between 250 and 400°C. The new technique of solid electrolyte potentiometry (SEP) was used to monitor the chemical potential of oxygen adsorbed on the metal catalyst. To this end the silver film catalyst also served as one of the electrodes of a solid electrolyte oxygen concentration cell and the open-circuit emf of the cell was monitored during reaction. It was found that the steady-state surface oxygen activity α_O is given by $a_O = P_{O_2}^{1/2}/(1 + K_{ETOX}P_{ETOX}^2)$, with $K_{ETOX} = 3.3 \cdot 10^{-5} \exp(10{,}600/T)$. This equation as well as the kinetics can be explained in terms of a simple reaction mechanism.

INTRODUCTION

Due to the industrial importance of the silver-catalyzed partial oxidation of ethylene to ethylene oxide, the mechanism of this reaction has been the subject of extensive study. Work prior to 1974 has been reviewed by Kilty and Sachtler (*1*).

In spite of the large number of investigations and some very interesting recent experimental findings (*2–6*), several important aspects of the reaction mechanism are still subject to controversy.

It is fairly well established that even with relatively short contact times part of the undesirable by-product CO_2 comes from the secondary oxidation of ethylene oxide (*1, 7, 8*). The kinetics and mechanism of the secondary oxidation of ethylene oxide to CO_2 and H_2O are the subjects of the present communication. The experimental approach was to combine kinetic studies in a CSTR with simultaneous *in situ* solid electrolyte aided measurement of the thermodynamic activity of oxygen on the working silver catalyst.

Although an understanding of the mechanism of this reaction is necessary for an understanding of the overall ethylene oxidation network, relatively few investigators have studied the ethylene oxide oxidation separately.

Twigg (*9*) found the rate of the reaction to be zero order in oxygen and first order in adsorbed ethylene oxide. He obtained an activation energy of 20 ± 5 kcal/mol and proposed that the rate-limiting step is the isomerization of adsorbed ethylene oxide to adsorbed acetaldehyde which is then rapidly oxidized to CO_2 and H_2O. He also reported formation of a strongly adsorbed organic deposit, possibly a "polymer of ethylene oxide" during reaction. Some evidence for adsorbed ethylene oxide oligomer formation has been found in recent ir studies of the ethylene oxidation (*6*).

More recent studies of the ethylene oxide oxidation on silver (*10–13*) have confirmed the zero-order dependence of the rate on P_{O_2}. Activation energies in good agreement with Twigg's value have been reported as well as zero- to first-order dependence on P_{ETOX}.

These observations can now be reexamined and reinterpreted in light of the directly measured thermodynamic activity a_O of oxygen adsorbed on the catalyst.

The new technique of solid electrolyte potentiometry (SEP) permits an *in situ* measurement of a_O on metal catalysts.

0021-9517/80/070018-11$02.00/0
Copyright © 1980 by Academic Press, Inc.
All rights of reproduction in any form reserved.

Originally proposed by Wagner (*14*), the technique utilizes a solid electrolyte oxygen concentration cell with one electrode also serving as the catalyst for the reaction under study. It has been used in conjunction with kinetic measurements to study the SO_2 oxidation on noble metals (*15*) and the ethylene oxidation on Ag (*16*) and Pt (*17*). An indirect measurement of the activity of oxygen on Ag catalysts during the oxidation of ethylene has been obtained by Imre (*18*). Solid electrolyte cells similar to the one described here were used by Mason and co-workers to enhance the rate of the NO catalytic decomposition on Pt by oxygen "pumping" (*19*). In the present study attention was focused on the open-circuit emf which permits direct calculation of a_O on the metal catalyst.

EXPERIMENTAL

The kinetic studies were carried out in a CSTR shown in Fig. 1. A schematic diagram of the overall apparatus is given in Fig. 2. The Ag catalyst film was deposited on the flat bottom of an 8% yttria-stabilized zirconia tube. To deposit the film a few drops of a silver suspension in butyl acetate (obtained from GC Electronics) was used followed by drying and calcining at 400°C. The surface of the silver catalyst was examined using AES and SEM. The surface area was estimated using oxygen chemisorption followed by reaction with ethylene and utilizing an infrared CO_2 analyzer. The same catalyst without any further pretreatment was also quite active and selective for the ethylene oxidation to ethylene oxide and its activity and selectivity remained fairly constant over a period of several weeks.

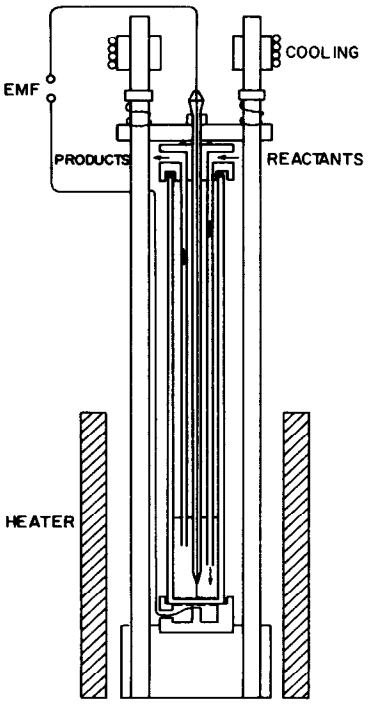

FIG. 1. Reactor cell configuration

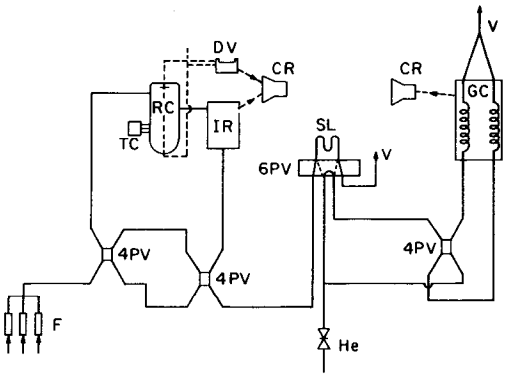

FIG. 2. Schematic diagram of the apparatus. (F) Calibrated feed flow meters, (4PV) four-port valve, (6PV) six-port valve, (RC) reactor cell, (TC) temperature controller, (IR) infrared CO_2 analyzer, (DV) differential voltmeter, (SL) sampling loop, (GC) gas chromatograph, (CR) strip-chart recorder, (V) vent.

A similar Ag film was deposited on the outside bottom wall of the stabilized zirconia tube. This Ag film was exposed to air and served as the reference electrode.

An appropriately machined stainless-steel cap was clamped to the open end of the tube. The cap had provision for introduction of reactants, removal of products as well as for introduction of an Ag wire, enclosed in a Pyrex tube to make contact with the internal Ag film catalyst-electrode.

The open-circuit emf of the oxygen concentration cell was measured with a J.

Fluke voltmeter with an input resistance of 10^8 ohms, and infinite resistance at null. The bottom of the stabilized zirconia tube was diamond polished to a thickness of ~200 μm so that the resistance of the oxygen concentration cell was below 1000 ohms even at the lowest temperatures used. The correct performance of the cell as an oxygen concentration cell was verified by introducing in the reactor various air–N_2 mixtures of known P_{O_2} and obtaining agreement within 1–2 mV with the Nernst equation

$$E = \frac{RT}{2F} \ln \frac{P_{O_2}^{1/2}}{0.21^{1/2}}.$$

The temperature of the reactor was controlled within 2°C by means of a Leeds and Northrup temperature controller and also measured with a second thermocouple touching the wall of the stabilized zirconia tube 1 mm from the reference electrode. Certified standard ethylene oxide mixtures in N_2 or CO_2 were mixed with zero gas air by means of a gas mixer. The reactants could be further diluted with N_2. The mixer flow meters were calibrated, in order to measure accurately the total flow rate.

The composition of reactants and products was determined by means of a Perkin–Elmer gas chromatograph with a TC detector. A Porapak Q column was used to separate air, CO_2, and ethylene oxide. A molecular sieve 5A column was used to separate N_2 and O_2. The carbon and oxygen balance between reactants and products was consistent within 1%. The concentration of CO_2 in the products was also directly monitored by a Beckman 864 ir analyzer.

RESULTS

Catalyst Characterization and Oxygen Desorption Experiments

The Auger spectrum of the used catalyst exhibited in Fig. 3 shows that the silver surface is fairly clean. Trace surface impurities include some Cl (probably less than

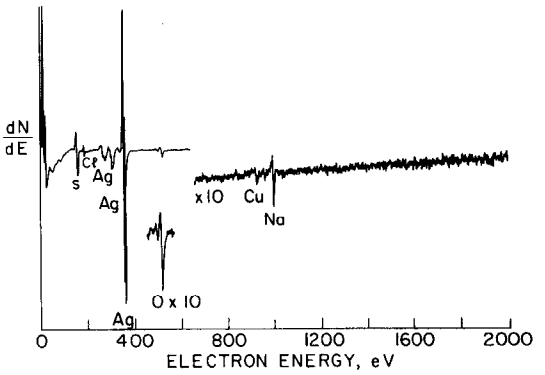

FIG. 3. Auger spectrum of the catalyst.

0.5% of a monolayer) which might be responsible to some extent for the observed high selectivity of this catalyst for the ethylene oxidation to ethylene oxide. A typical scanning electron micrograph of the catalyst is shown in Fig. 4.

The catalyst surface could adsorb approximately $2.0(\pm 0.8) \cdot 10^{-6}$ mol O_2. This was estimated as follows. Oxygen was allowed to chemisorb on the catalyst for at least 10 min at temperatures above 250°C. The reactor was then purged with ultrapure N_2 for a time t at least eight times longer than the residence time of the CSTR (~6 s) and then flushed with ethylene. The ir CO_2 analyzer was used to monitor continuously the O_2 concentration in the reactor effluent and thus determine the total number of CO_2 molecules formed by integrating the area of the very sharp peak obtained (peak width 5–8 s). The sharpness of the peak verified what was observed with independent steady-state ethylene oxidation experiments, i.e., that the kinetics of the ethylene oxidation to CO_2 are almost two orders of magnitude faster than the oxygen desorption kinetics. Since the ethylene oxidation selectivity of the catalyst was independently determined (*16*) and shown to be weakly dependent on residence time and gas-phase composition at given temperature, one may assume that the transient nature of these experiments introduces only small variations in selectivity, and thus estimate the amount of oxygen ad-

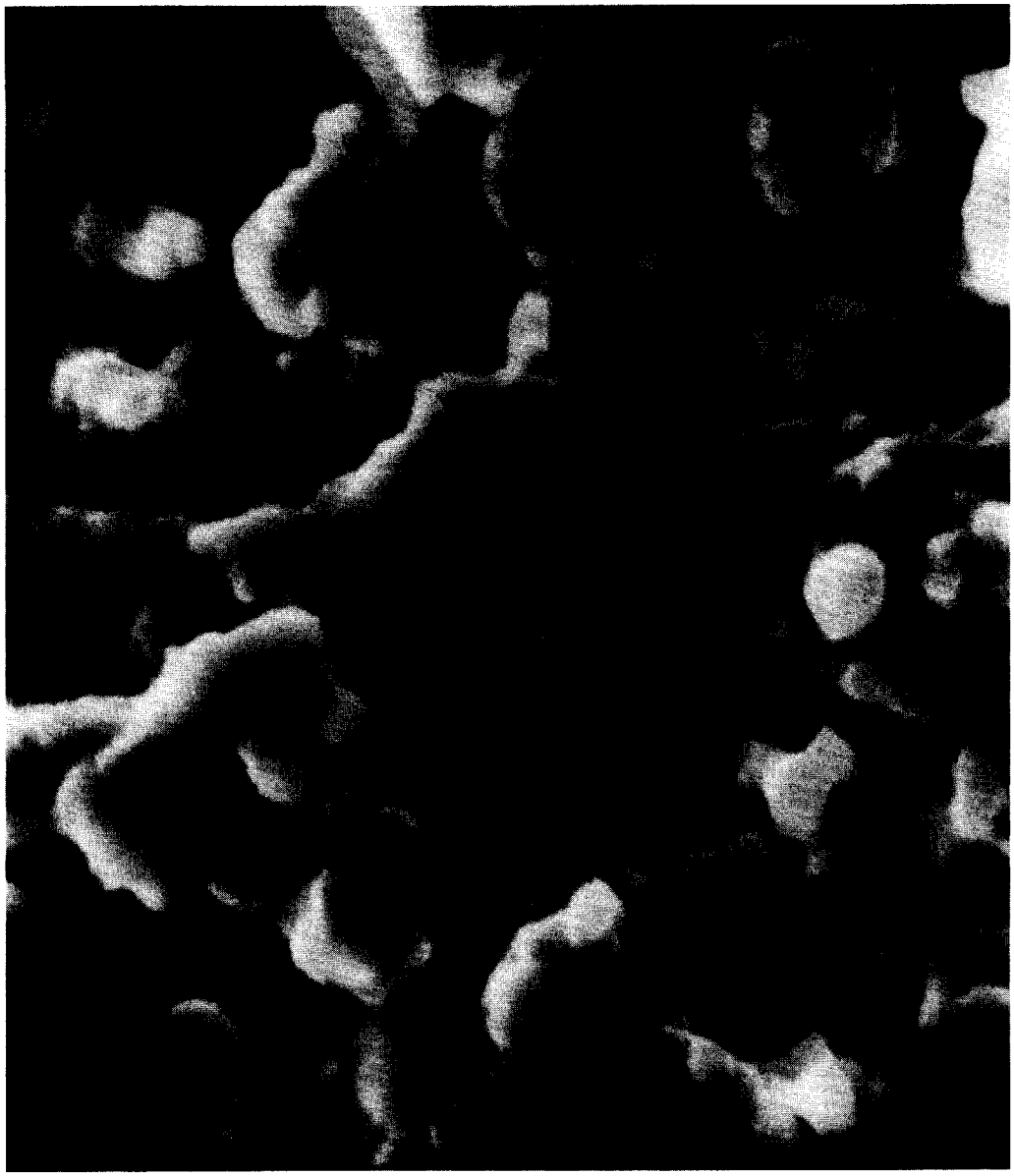

FIG. 4. Scanning electron micrograph of a catalyst sample.

sorbed on the catalyst at time t. By varying t one can examine the rate of oxygen desorption. A near-first-order dependence on adsorbed oxygen was observed (Fig. 5) so that the desorption rate R_{des} (moles of O_2 per second) can be expressed as

$$R_{des} = -K_2\theta_O.$$

The maximum number of moles of O_2 n_{O_2} adsorbed is found by extrapolating to $t = 0$. This can be used only as a rough estimate because of the considerable uncertainty introduced by the transient selectivity assumption. The estimated value is $2.0(\pm 0.8)$ 10^{-6} mol O_2 and is very weakly dependent on temperature. The values of K_2 thus obtained are compared in Table 2 with the rate coefficient K_R.

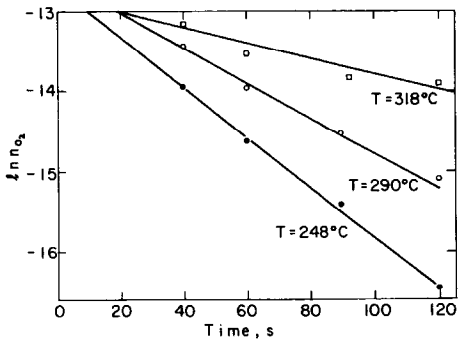

FIG. 5. Oxygen desorption experiments. Oxygen moles adsorbed (×2) vs time.

Kinetic Measurements

The reactor used in the present study has been shown to approximate very closely an ideal CSTR over similar space velocity conditions by using the ir CO_2 analyzer to obtain its residence time distribution function (*20*). The rate was calculated from the appropriate mass balance

$$r = F'(x_{C_2H_4O(\text{reactants})} - x_{C_2H_4O(\text{products})}),$$

where F' is the total molar flow rate and x is the mole fraction of ethylene oxide.

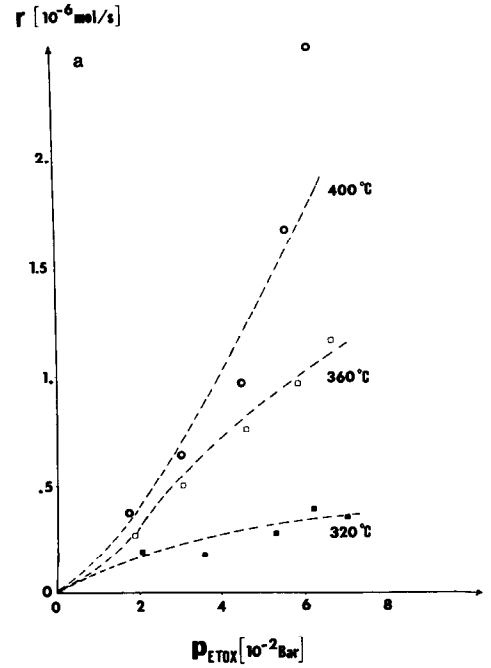

The rate is shown in Fig. 6a as a function of P_{ETOX} for three different temperatures. It is close to second order with respect to ethylene oxide at the higher temperatures studied, gradually changing to first order and almost zero order at temperatures below 300°C. The relevant kinetic data are given in Table 1. Each point is the average of two measurements.

The role of oxygen was investigated in a separate set of experiments by maintaining P_{ETOX} constant and varying P_{O_2}. The rate is zero order in oxygen as shown in Fig. 6b.

A simple first-order rate expression in ethylene oxide can describe the data at intermediate temperatures but is inadequate at the lower and higher temperatures studied. It was found that all the kinetic data could be expressed rather accurately by the rate expression

$$r = K_R \frac{K_{ETOX} P^2_{ETOX}}{1 + K_{ETOX} P^2_{ETOX}}, \qquad (1)$$

where

$$K_{ETOX} = 3.3 \cdot \exp\left(\frac{10{,}600}{T}\right) \text{bar}^{-2}$$

and

$$K_R = 14.4 \exp -\left(\frac{10{,}200}{T}\right)$$

g mol ETOX/s. (2)

In Fig. 6 the close agreement is shown between the rate expression (1) and the experimental data.

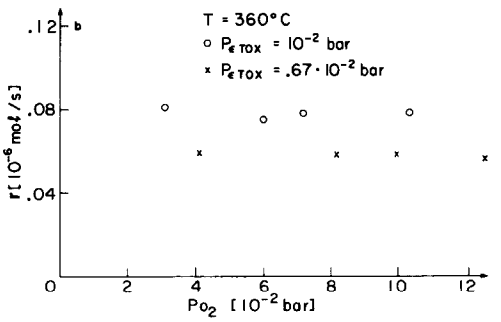

FIG. 6. (a) Rate vs P_{ETOX}. Dashed lines from Eqs. (1) and (2). (b) Rate vs P_{O_2} at constant P_{ETOX}.

TABLE 1

Kinetic and Potentiometric Results

Temperature (°C)	Total flow rate (cm^3 STP/min)	Reactants		Products		Open-circuit emf (mV)
		$100 \cdot X_{ETOX}$	$100 \cdot X_{O_2}$	$100 \cdot X_{ETOX}$	$100 \cdot X_{O_2}$	
400	100	2.27	16.17	1.75	14.86	−8.5
400	124	3.68	13.18	2.95	11.33	−14.5
400	160	5.30	9.74	4.53	7.80	−24.5
400	204	6.54	7.11	5.43	4.34	−37
400	260	7.40	5.27	6.07	1.93	−45
360	100	2.25	16.22	1.88	15.30	−10.5
360	124	3.68	13.17	3.16	11.88	−19
360	160	5.34	9.65	4.73	8.10	−32
360	204	6.50	7.18	5.90	5.66	−45.5
360	260	7.27	5.55	6.67	4.06	−62.5
320	100	2.27	16.17	2.01	15.50	−19.5
320	124	3.68	13.19	3.51	12.75	−33.5
320	160	5.39	9.55	5.17	9.00	−52.5
320	204	6.50	7.18	6.24	6.54	−66
320	260	7.23	5.64	7.06	5.22	−80
290	100	2.18	16.36	2.05	16.04	−29.5
290	124	3.68	13.17	3.59	12.94	−48.0
290	160	5.43	9.46	5.26	9.05	−71.5
290	204	6.50	7.18	6.37	6.85	−90.5
290	260	7.27	5.55	7.14	5.22	−107
260	100	2.31	16.08	2.20	15.80	−51.5
260	124	3.76	13	3.68	12.80	−75
260	160	5.43	9.46	5.39	9.36	−102.5

In a different set of experiments the effect of the CO_2 diluent was studied by replacing CO_2 with N_2 as the diluent and using partial pressures of ethylene oxide below 2%. It was found that the rate could still be fairly well described by Eq. (1) indicating (a) that CO_2 has an almost negligible retarding effect on the rate of the ethylene oxide oxidation and (b) that the rate expression (1) can be safely extrapolated to partial pressures of ethylene oxide well below 0.02 bar, although it was derived by fitting kinetic data obtained with P_{ETOX} varying between 0.02 and 0.08 bar.

In Situ Surface Oxygen Activity Measurements

The open-circuit emf as measured using the new technique of solid electrolyte potentiometry (SEP) is also given in Table 1. The surface oxygen activity a_O is defined by

$$\mu_{O_2(Ag)} = \mu^0_{O_2(g)} + RT \ln a^2_{O(Ag)} \qquad (3)$$

so that $a^2_{O(Ag)}$ expresses the partial pressure of oxygen gas that would be in thermodynamic equilibrium with oxygen adsorbed on silver, if such an equilibrium were established.

The defining equation (3) of the activity a_O of surface oxygen atoms does not imply that oxygen adsorbs in the form of atoms only. It is fairly well established that several forms of adsorbed oxygen exist on silver (*1*). To the extent that these various forms of adsorbed oxygen are in thermodynamic equilibrium, i.e., they all have the same steady-state chemical potential, then the emf measurements reflect this common chemical potential. If, however, such an equilibrium is not established, then the emf reflects the activity of oxygen atoms (*14*), as they are the fastest ones to equilibrate

with the O^{2-} of the stabilized zirconia. This is further discussed below.

As mentioned before, it was observed experimentally that indeed

$$a_{O(Ag)}^2 = P_{O_2(g)} \qquad (4)$$

when O_2–inert gas mixtures were introduced in the reactor. However, in the presence of ethylene oxide in the reactor, i.e., under reaction conditions, Eq. (4) is not satisfied anymore and in general

$$a_{O(Ag)}^2 < P_{O_2(g)}$$

although at high temperatures and low partial pressures of ethylene oxide, $a_{O(Ag)}^2$ approaches very closely to P_{O_2}. Several functional forms were examined for the dependence of a_O on gas-phase composition. It was found that the a_O measurements (i.e., the emf data) could be very well correlated in terms of the equation

$$\frac{P_{O_2}^{1/2}}{a_O} - 1 = K_{ETOX} P_{ETOX}^2. \qquad (5)$$

This is shown in Fig. 7. It should be noted that

(a) If the left side of Eq. (5) were equal to zero, i.e., $P_{O_2}^{1/2} = a_O$, that would imply equilibration between surface oxygen and gas-phase oxygen during reaction. This is not true except at very high temperatures and very low values of P_{ETOX}.

(b) The same parameter $K_{ETOX} = 3.3 \cdot 10^{-5} \exp(10{,}600/T)$ obtained from the kinetic data is the crucial parameter for the description of the surface oxygen activity measurements and corresponds to the slopes of the straight lines of Fig. 7. The temperature dependence of K_R and K_{ETOX} is shown in Figs. 8 and 9.

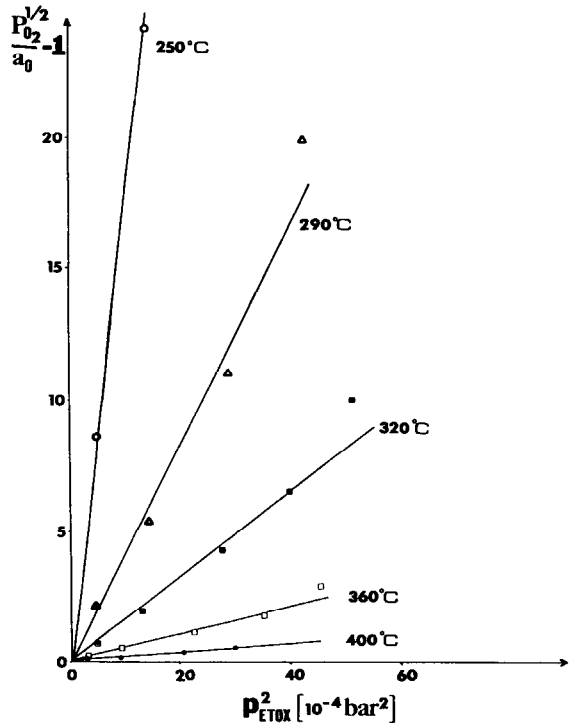

FIG. 7. Surface oxygen activity dependence on gas-phase composition.

DISCUSSION

It was proposed by Twigg many years ago (*8*, *9*) that the rate-limiting step of the silver-catalyzed ethylene oxide oxidation is the isomerization of adsorbed ethylene oxide to acetaldehyde which is then rapidly oxidized by surface or gas-phase oxygen to CO_2 and H_2O. This classical picture can now be reexamined in light of the *in situ* surface oxygen activity measurements.

Any proposed mechanism for the oxidation of ethylene oxide on silver should be able to explain (i) the surface oxygen activity behavior (Eq. 5), (ii) the observed rate expression (Eq. 1), and (iii) the observation that the same temperature-dependent parameter K_{ETOX} appears both in the rate expression and the oxygen activity equation.

These three requirements decrease the possible mechanisms to a very small number.

First, the inequality

$$a_O^2 < P_{O_2}$$

shows that thermodynamic equilibrium is not established between surface and gas-phase oxygen during reaction. This implies that either oxygen adsorption is rate limiting in the classical sense or that the rate of oxygen adsorption and desorption is com-

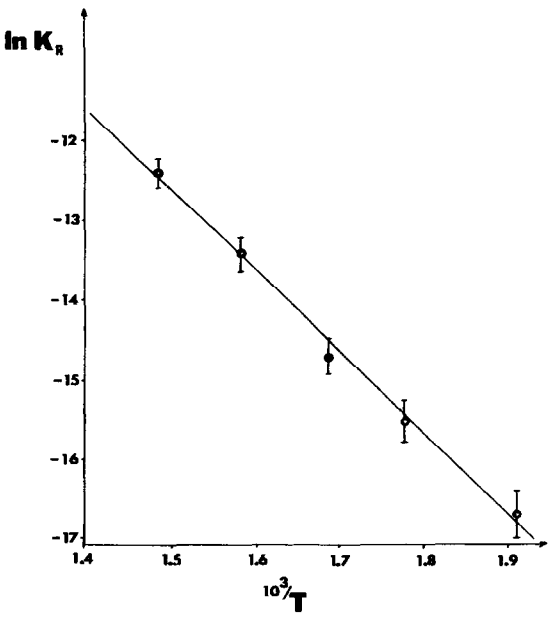

FIG. 8. Temperature dependence of K_R.

parable with the rate of the oxidation step. The first possibility can be ruled out in light of the rate expression (Eq. 1). Therefore the reaction rate is of the same order of magnitude with the intrinsic rate of oxygen adsorption on silver.

Both experimental equations (1) and (5) very strongly suggest adsorbed ethylene oxide dimer formation. This is not surprising in view of the previous work of Twigg (*8*, *9*) and Force and Bell (*6*). The rate expression clearly shows that adsorbed ethylene oxide dimer rather than gaseous ethylene oxide is involved in the oxidation step. Furthermore the fact that $a_O^2 < P_{O_2}$ shows that adsorbed ethylene oxide reacts with adsorbed oxygen rather than gaseous oxygen. Therefore the results are very strongly indicative of a Langmuir–Hinshelwood rather than Rideal–Eley type mechanism.

The question can be addressed of whether the rate-limiting step is the isomerization of adsorbed ethylene oxide dimer to a highly reactive isomer which then reacts with adsorbed oxygen to form CO_2 and H_2O according to Twigg's mechanism. Although the rate expression can thus be accounted for, we found it impossible to interpret the surface oxygen activity behavior on the basis of such a rate-limiting step. However, we found that the following mechanism could explain all the experimental observations:

$$\tfrac{1}{2}\{O_2(g) \rightleftarrows 2O^*\}, \quad (6)$$

$$O^* + S_1 + S_2 \rightarrow O - S_2 + S_1, \quad (6a)$$

$$2C_2H_4O + S_1 \rightarrow C_4H_8O_2 - S_1, \quad (7)$$

$$O - S_2 + C_4H_8O_2 - S_1 \rightarrow P \xrightarrow{9[O]} 4CO_2 + 4H_2O + S_1 + S_2, \quad (8)$$

where P stands for a highly reactive intermediate which is rapidly oxidized to CO_2 and H_2O, and O* stands for oxygen in a precursor adsorption state. Postulating this precursor state is necessary in order to account for the a_O behavior (Fig. 7) as shown below. The assumption of two different types of surface sites S_1 and S_2 was found necessary in order to account quanti-

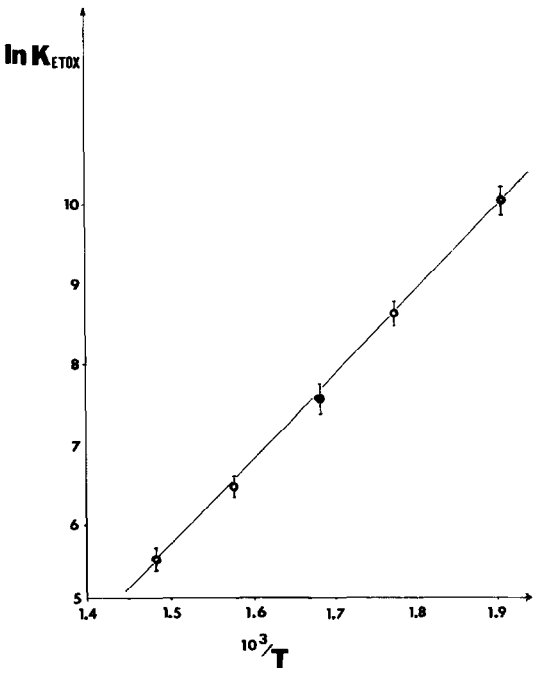

FIG. 9. Temperature dependence of K_{ETOX} obtained from the SEP data.

tatively for the experimental observations (1) and (5).

Quantitative Kinetics

On the basis of the above mechanism and with the additional assumption of Langmuir-type adsorption one can explain all the experimental observations in a quantitative manner. This may not be the only possible interpretation, but it is the simplest one we could find.

Since step (7) is in thermodynamic equilibrium one obtains

$$\theta_{ETOX} = \frac{K_{ETOX}P^2_{ETOX}}{1 + K_{ETOX}P^2_{ETOX}}, \qquad (9)$$

where θ_{ETOX} is the coverage of surface sites S_1 by ethylene oxide dimer. Therefore K_{ETOX} is the adsorption coefficient of ethylene oxide on silver and one can directly obtain the heat and entropy of chemisorption of ethylene oxide from Eq. (2).

$$\Delta H_{ETOX} = -88{,}000 \text{ J/mol dimer} = -44{,}000 \text{ J/mol ETOX}$$

$$\Delta S_{ETOX} = -85.8 \text{ J/K} \cdot \text{mol dimer} = -42.9 \text{ J/K} \cdot \text{mol ETOX}.$$

At steady state the difference between the rates of oxygen adsorption and desorption equals the rate of reaction and according to steps (6) and (6a) one obtains

$$K_1P^{1/2}_{O_2}(1 - \theta_{ETOX})(1 - \theta_O) - K_2\theta_O(1 - \theta_{ETOX}) = K_R\theta_O\theta_{ETOX}, \qquad (10)$$

where K_1 and K_2 are rate coefficients and $K_1/K_2 \equiv K_O$ is the adsorption coefficient of atomic oxygen. In the absence of chemical reaction ($K_R = 0$) Eq. (10) reduces to the common form of the Langmuir isotherm

$$K_OP^{1/2}_{O_2} = \frac{\theta_O}{1 - \theta_O}. \qquad (11)$$

Since a_O expresses the square root of the partial pressure of gaseous oxygen that would be in thermodynamic equilibrium with adsorbed oxygen at coverage θ_O if such an equilibrium were established, it follows that

$$K_Oa_O = \frac{\theta_O}{1 - \theta_O} \qquad (12)$$

even when gaseous–surface oxygen equilibration is not established. Combining Eqs. (9), (10), and (12) one obtains

$$\frac{P^{1/2}_{O_2}}{a_O} - 1 = \frac{K_R}{K_2}K_{ETOX}P^2_{ETOX}. \qquad (13)$$

On the basis of the mechanism (step (6a)) desorption of oxygen requires the existence of an adjacent empty site S_1, i.e., the rate-limiting step for oxygen desorption is O migration from an S_2 to an S_1 site. Therefore K_2 is the rate coefficient for this elementary step. If the adjacent S_1 site is occupied by ethylene oxide, reaction occurs. Therefore K_R is the rate coefficient for the same elementary step of O migration from an S_2 to an S_1 site, so that

$$K_R = K_2. \qquad (14)$$

This is supported by the oxygen desorption experiments from ethylene oxide free silver catalyst (Table 2).

In light of (14), Eq. (13) reduces to the experimental equation

$$\frac{P^{1/2}_{O_2}}{a_O} - 1 = K_{ETOX}P^2_{ETOX}. \qquad (5)$$

The implication of (14) is that the measurable K_R (Eq. (2)) is in essence the rate coefficient for atomic oxygen desorption, so that the activation energy for atomic oxygen desorption is 85 kJ/g-atom O, $\Delta E^*_{DES\ O} = 85$ kJ/g-atom O, and $\Delta S^*_{DES\ O} \approx -125$ J/K g-atom O. This activation energy is in reasonable agreement with reported literature values (*1*).

TABLE 2

Oxygen Desorption and Ethylene Oxide Oxidation Rate Coefficients

Temperature (°C)	K_2 (mol/s)	K_R (mol/s)
248	$5.1 \cdot 10^{-8}$	$4.3 \cdot 10^{-8}$
290	$8.5 \cdot 10^{-8}$	$18 \cdot 10^{-8}$
318	$12.9 \cdot 10^{-8}$	$44.5 \cdot 10^{-8}$

Finally the rate equation

$$R = K_R\theta_O\theta_{ETOX} = K_R \frac{K_O a_O}{1 + K_O a_O} \cdot \frac{K_{ETOX}P^2_{ETOX}}{1 + K_{ETOX}P^2_{ETOX}}$$

reduces to the experimental rate expression (1) if $K_O a_O \gg 1$ which implies that most of the S_2 sites are occupied by O atoms during reaction, i.e., $\theta_O \sim 1$ which is quite reasonable under atmospheric pressure conditions. It should be noted that θ_O is insensitive to changes in a_O to the extent that $a_O \gg K_O^{-1}$ (Eq.(12)). Practically all the previously reported rate expressions reviewed in (*13*) can be considered as limiting cases of the rate expression (1). The activation energy found is in reasonable agreement with previously reported values (*9*, *13*). That no second-order dependence of the rate on P_{ETOX} has been reported is readily explained by noticing that all the previous kinetic studies were restricted to operating temperatures below 350°C. The present results should not be taken to imply that atomic oxygen is the only form of oxygen adsorbed on silver. They show, however, that adsorbed atomic oxygen is responsible for the oxidation of ethylene oxide.

SUMMARY

The kinetics of the ethylene oxide oxidation on polycrystalline silver films were studied in a CSTR at atmospheric pressure in conjunction with simultaneous *in situ* solid electrolyte aided measurement of the thermodynamic activity of oxygen on the catalyst. It was found that

(a) The surface oxygen activity does not generally equal the gas-phase oxygen activity except at high temperatures and vanishing P_{ETOX}. It satisfies the equation $a_O = P_{O_2}^{1/2}/(1 + K_{ETOX}P^2_{ETOX})$.

(b) The reaction rate can be described by

$$R = K_R K_{ETOX} P^2_{ETOX}/(1 + K_{ETOX}P^2_{ETOX}).$$

(c) K_R is also very close to the rate coefficient for oxygen desorption from the silver surface.

These results strongly indicate that

(i) Adsorbed atomic oxygen is responsible for the ethylene oxide oxidation.

(ii) Atomic oxygen and ethylene oxide adsorb on two different types of surface sites S_2 and S_1, respectively. Ethylene oxide adsorbs as a dimer.

(iii) The rate-limiting step is migration of atomic oxygen from an S_2 to an S_1 site. If the site is occupied by ethylene oxide, oxidation occurs. If not, oxygen desorption takes place.

The present results should be useful for a better understanding of the overall reaction network of the ethylene oxidation on silver. They also show the usefulness of solid electrolyte potentiometry as a tool for the study of catalytic oxidations on metals.

ACKNOWLEDGMENTS

This research was supported under NSF Grant ENG 77-27500. Acknowledgment is also made to the Donors of the PRF for partial support of this research under Grant 9893-G3.

REFERENCES

1. Kilty, P. A., and Sachtler, W. M. H., *Catal. Rev. Sci. Eng.* **10**(1), 1 (1974).
2. Kilty, P. A., Rol, N. C., and Sachtler, W. M. H., *in* "Proceedings, 5th International Congress on Catalysis, Palm Beach, 1972" (J. W. Hightower, Ed.), Paper 64, p. 929. North-Holland, Amsterdam, 1973.
3. Carberry, J. J., Kuczynski, G. C., and Martinez, E., *J. Catal.* **28**, 39 (1973).
4. Cant, N. W., and Hall, W. K., *J. Catal.* **52**, 81 (1978).
5. Larrabee, A. L., and Kuczkowski, R. L., *J. Catal.* **52**, 72 (1978).
6. Force, E. L., and Bell, A. T., *J. Catal.* **40**, 356 (1975).
7. Voge, H. H., and Adams, C. R., *in* "Advances in Catalysis and Related Subjects" (D. D. Eley, H. Pines, and P. B. Weisz, Eds.), Vol. 17, p. 151. Academic Press, New York, 1967.
8. Twigg, G. H., *Proc. Roy. Soc. London Ser. A* **188**, 92 (1946).
9. Twigg, G. H., *Trans. Faraday Soc.* **42**, 284 (1946).
10. Rubanik, M. Y., *et al., Dokl. Akad. Nauk. Ukr. SSR*, 2 (1949).
11. Margolis, Y., and Roginski, S. Z., *Probl. Kinet. Katal. Akad. Nauk SSR* **9**, 107 (1957).
12. Kenson, R. E., and Lapkin, M., *J. Phys. Chem.* **74**, 7, 1493 (1970).

13. Ionov, Y. V., *et al.*, *Zh. Phis. Khim.* (*Leningrad*) **44**(3), 609 (1971).
14. Wagner, C., *in* "Advances in Catalysis and Related Subjects" (D. D. Eley, H. Pines, and P. B. Weisz, Eds.), Vol. 21, p. 323. Academic Press, New York, 1970.
15. Vayenas, C., and Saltsburg, H., *J. Catal.* **57**, 296 (1979).
16. Vayenas, C., and Stoukides, M., in preparation.
17. Vayenas, C., Lee, B., and Michaels, J., accepted for publication, *J. Catal.* (1980).
18. Imre, L., *Ber. Bunsenges. Phys. Chem.* **74**, 220 (1970).
19. Pancharatnam, S., Huggins, R. A., and Mason, D. M., *J. Electrochem. Soc.* **122**, 869 (1975).
20. Lee, B., M.S. Thesis, M.I.T., 1979.